

Resveratrol attenuates doxorubicin-induced cardiomyocyte apoptosis in mice through SIRT1-mediated deacetylation of p53

Chi Zhang^{1,2}, Yansheng Feng¹, Shunlin Qu^{1,2}, Xing Wei^{1,2}, Honglin Zhu¹, Qi Luo¹, Meidong Liu¹, Guangwen Chen¹, and Xianzhong Xiao^{1*}

¹Department of Pathophysiology, Xiangya School of Medicine, Central South University, 110 Xiangya Road, Changsha, Hunan 410078, People's Republic of China; and ²Institute of Cardiovascular Disease, Key Laboratory for Arteriosclerosis of Hunan Province, University of South China, 28 Changshengxi Road, Hengyang, Hunan 421001, People's Republic of China

Received 15 July 2010; revised 11 January 2011; accepted 19 January 2011; online publish-ahead-of-print 27 January 2011

Time for primary review: 39 days

Aims	Doxorubicin (DOX) is an anthracycline drug with a wide spectrum of clinical antineoplastic activity, but increased apoptosis has been implicated in its cardiotoxicity. Resveratrol (RES) was shown to harbour major health benefits in diseases associated with oxidative stress. In this study, we aimed to determine the effect of RES on DOX-induced myocardial apoptosis in mice.
Methods and results	Male Balb/c mice were randomized to one of the following four treatments: saline, RES, DOX, or RES plus DOX (10 mice in each group). DOX treatment markedly depressed cardiac function, decreased the heart weight, the body weight, and the ratio of heart weight to body weight, but inversely increased the level of protein carbonyl, malondialdehyde, and serum lactate dehydrogenase, and induced mitochondrial cytochrome c release and cardiomyocyte apoptosis. However, these effects of DOX were ameliorated by its combination with RES. Further studies with a co-immunoprecipitation assay revealed an interaction between p53 and Sirtuin 1 (SIRT1). It was found by western blot and electrophoretic mobility shift assay that DOX treatment increased p53 protein acetylation and cytochrome c release from mitochondria, activated p53 binding at the <i>Bax</i> promoter, and up-regulated <i>Bax</i> expression, but supplementation with RES could weaken all these effects.
Conclusion	The protective effect of RES against DOX-induced cardiomyocyte apoptosis is associated with the up-regulation of SIRT1-mediated p53 deacetylation.
Keywords	Resveratrol • Doxorubicin • SIRT1 • p53 • Apoptosis

1. Introduction

Doxorubicin (DOX) is the mainstay of treatment for various haematological malignancies and solid tumours. However, its clinical benefit is limited by cumulative dose-related cardiotoxicity, which may ultimately lead to a severe and irreversible form of cardiomyopathy. Previous studies demonstrated that apoptosis plays an important role in doxorubicin-induced cardiotoxicity.^{1,2} Resveratrol (RES), a polyphenol found in red wine, possesses comprehensive biochemical and physiological actions, including antiplatelet and anti-inflammatory properties. Recent studies revealed the cardioprotective abilities of RES in both acute and chronic models.^{3–5} In addition, RES lowers the

Michaelis constant of Sirtuin 1 (SIRT1), a mammalian homologue of the *Saccharomyces cerevisiae* chromatin silent information regulator Sir2, and increases the cell survival by stimulating SIRT1-dependent deacetylation of p53.⁶

In this study, we tested whether RES, through increasing SIRT1 activity, could modulate p53 functions *in vivo* and ultimately impact on the regulation of cardiomyocyte apoptosis. Our data revealed that RES treatment in experimental mice attenuated DOX-induced cardiomyocyte apoptosis, alleviated the cardiotoxicity, preserved cardiac function, suppressed the release of cytochrome c from mitochondria, and decreased the level of acetylated p53 and p53-dependent transcription of *Bax*.

* Corresponding author. Tel: +86-731-82355019, Fax: +86-731-82355019, Email: xianzhongxiao@xysm.net

2. Methods

2.1 Animals and treatment

Male wild-type Balb/c mice, 8 weeks old, were purchased from the Animal Center, Central South University, Changsha, China. The mice were housed in a temperature- and humidity-controlled animal house at 25°C with a 12 h–12 h light–dark cycle. The mice were randomized into four groups (10 mice each) with similar body weight, as follows: a normal diet-fed group (control), a normal diet plus RES group (RES), a DOX (Sigma-Aldrich Co., St Louis, MO, USA) treatment group (DOX), and a DOX-supplemented RES group (R + D). In each of the DOX-treated groups, DOX at a dose of 8 mg/kg was injected intraperitoneally into the mice at 3 week intervals (cumulative dose of 24 mg/kg). In each of the RES-treated groups, RES was incorporated into mouse standard chow at 0.01% (w/w). In this way, mice obtained a RES intake of approximately 15 mg/kg each day. Control mice were injected with the same volume of sterile isotonic saline. All mice were killed 7 weeks after the initial injection.

The investigation followed the *Guide for the Care and Use of Laboratory Animals* published by the US National Institutes of Health (NIH publication no. 85-23, revised in 1996) and the Animal Care and Use Committee of Central South University. The study protocol was approved by the Ethics Committee of Central South University, Medical Institution Animal Care and Research Advisory Committee (Changsha, China).

2.2 Cardiac haemodynamic measurements

Seven weeks after DOX administration, left ventricular (LV) performance was measured in mice anaesthetized with intraperitoneal injections of 10% chloral hydrate (2.5 mL/kg). The mice were placed on controlled heating pads, and the core temperature, measured via a rectal probe, was maintained at 36–38°C. According to a previously described method,⁷ a small cannula filled with heparin saline (500 U/mL) was inserted into the left ventricle through the apex with the chest open and mechanically ventilated, and positioned along the cardiac longitudinal axis. After stabilization for 2 min, the pressure signal was continuously recorded using a MacLab A/D converter (AD Instruments, Mountain View, CA, USA). The left ventricular systolic and end-diastolic pressures were measured, and the maximal slope of systolic pressure increment (+dP/dt) and diastolic pressure decrement (–dP/dt) were calculated. After the haemodynamic measurements were made, the mice were killed.

2.3 Serum lactate dehydrogenase measurement

After DOX treatment, the mice were killed, and blood was drawn from the vena cava inferior. The blood samples were allowed to clot, and the serum was used for the measurement of lactate dehydrogenase (LDH) activities. LDH activities were determined with a kit (Nanjing Jiancheng Biotechnology Institute, Nanjing, Jiangsu, China) according to the manufacturer's instructions and expressed as units per litre.

2.4 Protein carbonyl content

Cardiac protein carbonyl (PC) content was determined spectrophotometrically by a method based on the reaction of the carbonyl group with 2,4-dinitrophenylhydrazine to form 2,4-dinitrophenylhydrazone,⁸ and the values were expressed as nanomoles of carbonyl per milligram of protein.

2.5 Lipid peroxidation

Lipid peroxidation products were determined by measuring malondialdehyde (MDA) content in tissue homogenates according to the method described previously.⁸ The MDA content was measured spectrophotometrically at 532 nm and calculated based on a standard curve using 1,1,3,3-tetraethoxypropane as a standard. Values were expressed as nanomoles per gram of protein.

2.6 Apoptosis assessment by TUNEL assay

To detect apoptosis, TUNEL (terminal deoxynucleotide transferase-mediated dUTP nick end labelling) staining was performed using In Situ Cell Apoptosis Detection Kits (Boster Biological Technology, Wuhan, Hubei, China). According to the manufacturer's instructions, paraffin-embedded sections of samples were deparaffinated and hydrated, and then incubated in 20 g/mL protease K at room temperature for 5 min. After being washed twice, the samples were put into sodium citrate buffer (2 mmol/L citric acid, and 10 mmol/L trisodium citrate, pH 6.0) at 37°C for 5 min. After being washed with phosphate-buffered saline (PBS) for 5 min twice, 20 µL TUNEL reaction mixture (1 µL terminal deoxynucleotidyl transferase, 1 µL digoxin-labelled d-UTP and 18 µL Labelling Buffer) was added to the sample, and incubated at 37°C for 60 min. After rinsing, the sections were incubated with biotin–anti-digoxin antibody for 30 min at 37°C and developed with DAB Substrate Kit. The slides were lightly counterstained with haematoxylin and then dehydrated and mounted. For each myocardial specimen, tissue sections were examined microscopically at ×400 magnification, and 10 random fields per section were counted. The percentage of apoptotic cells was calculated by the apoptotic index, i.e. dividing the number of positive-staining myocyte nuclei by the total number of myocyte nuclei.

2.7 Protein preparation and western blot

Proteins from the heart tissues were extracted in RIPA buffer (1% Triton X-100, 150 mmol/L NaCl, 5 mmol/L EDTA, and 10 mmol/L Tris-HCl, pH 7.0) containing a protease inhibitor cocktail. Protein extracts were subjected to centrifugation at 13 200 g for 10 min. Total protein (10–50 µg per lane) was electrophoresed and separated on a 10% SDS–polyacrylamide gel and transferred to a polyvinylidene fluoride membrane (Millipore, Billerica, MA, USA), which was soaked in 5% bovine serum albumin in Tris-buffered saline Tween (TBST, pH 7.6). The membrane was incubated overnight with a rabbit polyclonal antibody to SIRT1 (Millipore, Billerica, MA, USA) at a dilution of 1:500, or a mouse monoclonal antibody to p53 (Santa Cruz Biotechnology, Santa Cruz, CA, USA) at a dilution of 1:200, or a rabbit polyclonal antibody to Bax (Cell Signaling Technology, Danvers, MA, USA) at a dilution of 1:400 on a rotating platform at 4°C. Subsequently, the membrane was rinsed in TBST (pH 7.6) and incubated with horseradish peroxidase-conjugated IgG antibodies diluted in TBST (1:2000) for 2 h on a rotating platform at 4°C. Bands were visualized using a horseradish peroxidase developer, and background-subtracted signals were quantified on a laser densitometer (Bio-Rad, Hercules, CA, USA). Blots were probed with rabbit monoclonal antibody to glyceraldehyde 3-phosphate dehydrogenase (GAPDH; Cell Signaling Technology, Danvers, MA, USA) to ensure equal protein loading. All protein levels were assessed by densitometry with GAPDH as a control.

2.8 Co-immunoprecipitation

Frozen left ventricle was rapidly homogenized in RIPA buffer [10 mmol/L Tris-Cl, 1 mmol/L EDTA, 0.5 mmol/L EGTA, 140 mmol/L NaCl, 1% (v/v) Triton X-100, 0.1% sodium deoxycholate, 0.1% sodium dodecyl sulfate, and 1 mmol/L phenylmethylsulfonyl fluoride). Protein (500 µg) was pre-cleared with Protein G Plus/Protein A Agarose Suspension (Calbiochem, San Diego, CA, USA) and then incubated with 4 µg antibody (SIRT1 or p53) at 4°C overnight. After the incubation, the reaction mixture was gently rocked by adding 100 µL Protein G Plus/Protein A Agarose Suspension at 4°C for 4 h. We collected the agarose beads by centrifugation, and drained off the supernatant. Finally, protein agarose beads were washed with RIPA buffer, boiled for 5 min in 2 × SDS sample buffer, and frozen until used for western blot.

2.9 Acetylation assay

Left ventricle homogenate was subjected to immunoprecipitation with a p53 antibody, and acetylated p53 was detected by western blot with an acetylated lysine antibody (Cell Signaling Technology, Danvers, MA, USA).

2.10 Electrophoretic mobility shift assay

The DNA-binding activity of p53 was evaluated by electrophoretic mobility shift assay (EMSA). According to the manufacturer's instructions (LightShift chemiluminescent EMSA kit; Pierce, Rockford, IL, USA), nuclear proteins were isolated using the method described previously.⁹ Protein concentrations were measured by BCA Protein Assay Reagents (Pierce, Rockford, IL, USA) with bovine serum albumin (BSA) as a standard. Protein–DNA binding was carried out in a final volume of 40 μ L. In each tube, 4 μ L 10 \times binding buffer (100 mmol/L Tris, pH 8.0, 10 mmol/L EDTA, 40% glycerol, and 1 mol/L NaCl), 100 ng 1,4-dithiothreitol (DTT), 4 μ g BSA, 2 μ g dl-dC, and 30 μ g nuclear proteins were added. After the samples had been incubated at room temperature for 10 min, 1 μ L biotin-labelled p53-responsive portion of the *Bax* promoter 5'-GAT CCT CAC AAG TTA GAG ACA AGC CTG GGC GTG GGC TAT ATT G-3' was added to each reaction and incubated for 20 min at room temperature. The sample was resolved on 5% acrylamide gel in 0.25 \times Tris-borate-EDTA buffer.

2.11 Isolation of mitochondria and cytochrome c assay

The isolated hearts were washed in sterile PBS and the mitochondria were isolated according to the manufacturer's instructions (Mitochondria Isolation Kit for Tissue; Pierce, Rockford, IL, USA). Briefly, tissues were minced after addition 800 μ L Mitochondria Isolation Reagent A and carefully homogenized with 20 strokes on ice. The crude homogenates then were returned to the original tube, and 800 μ L Mitochondria Isolation Reagent C was added. The tube was centrifuged at 700 *g* for 10 min at 4°C. The supernatant was transferred and centrifuged at 3000 *g* for 15 min at 4°C to obtain a more purified fraction of mitochondria. The resulting supernatant was transferred into a new tube and centrifuged at 12 000 *g* to produce a more purified cytosolic fraction and saved for cytochrome c assay. The pellet contained the isolated mitochondria. Mitochondria Isolation Reagent C (500 μ L) was added to the pellet, and the mixture was centrifuged at 12 000 *g* for 5 min. The mitochondrial pellet was resuspended in 300 μ L of mitochondria isolation buffer containing 0.1% Triton X-100 and protease inhibitors. Protein concentrations of both mitochondrial and cytosolic lysates were determined using BCA Protein Assay Reagents (Pierce, Rockford, IL, USA). To detect cytochrome c release into the cytosol, western blotting was performed with anti-cytochrome c antibody (Abcam) diluted 1:2000 in 1% (w/v) bovine serum albumin in PBS buffer. Voltage-dependent anion channel (VDAC), a mitochondrial marker, was also detected by western blot.

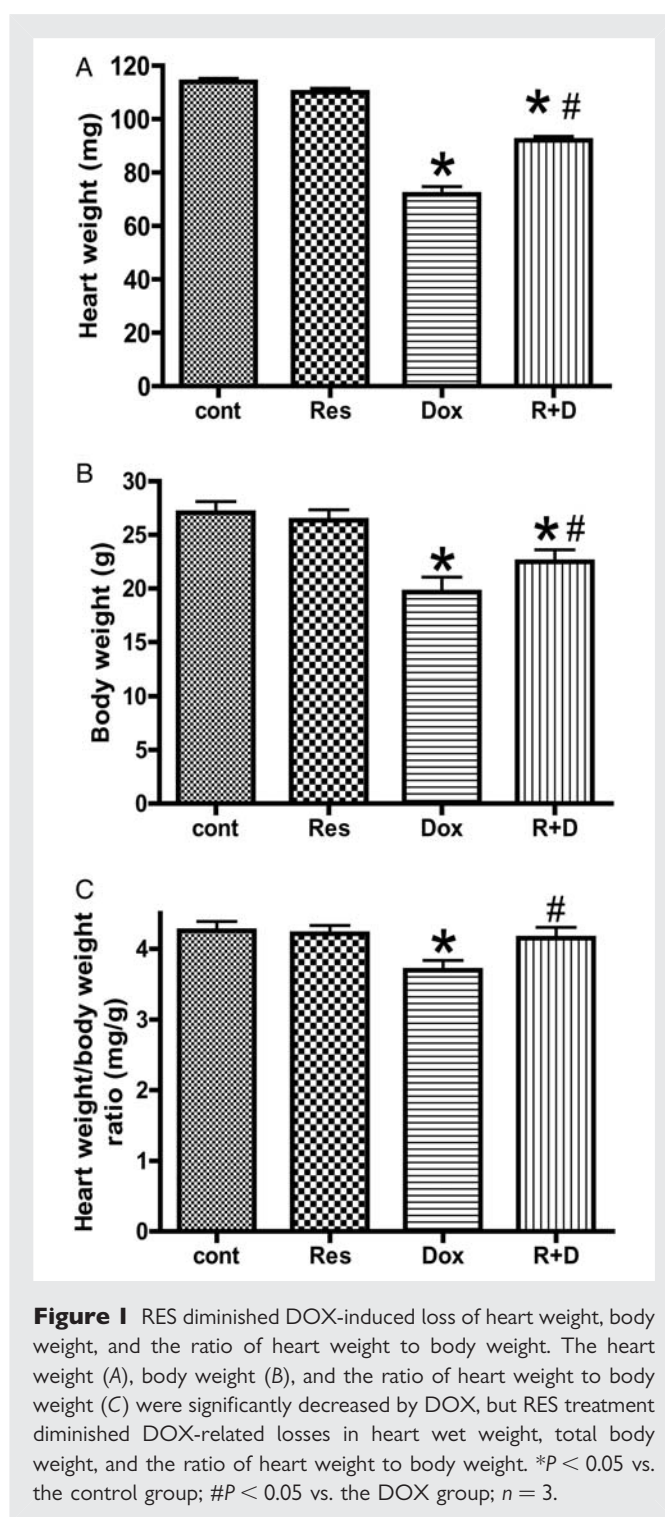
2.12 Statistical analysis

All the quantitative data are presented as means \pm SD and compared by one-way ANOVA. A level of $P < 0.05$ was considered statistically significant.

3. Results

3.1 RES diminished DOX-induced loss of heart weight, body weight and the ratio of heart weight to body weight

The heart weight, body weight and the ratio of heart weight to body weight were significantly ($P < 0.05$) decreased by DOX treatment (Figure 1), but RES treatment diminished DOX-induced losses in heart wet weight and total body weight by 47.9 ($P < 0.05$; Figure 1A) and 32.2% ($P < 0.05$; Figure 1B), respectively. The decrease in the ratio of heart weight to body weight due to DOX treatment



was also alleviated by RES in the R + D group compared with the DOX group ($P < 0.05$; Figure 1C).

3.2 RES attenuated DOX-induced LV dysfunction

Haemodynamic measurements were recorded to determine the protective effect of RES on LV function in DOX-treated mice. We discovered no significant difference in the haemodynamic indices between the control and RES groups, but the mice treated with DOX had a

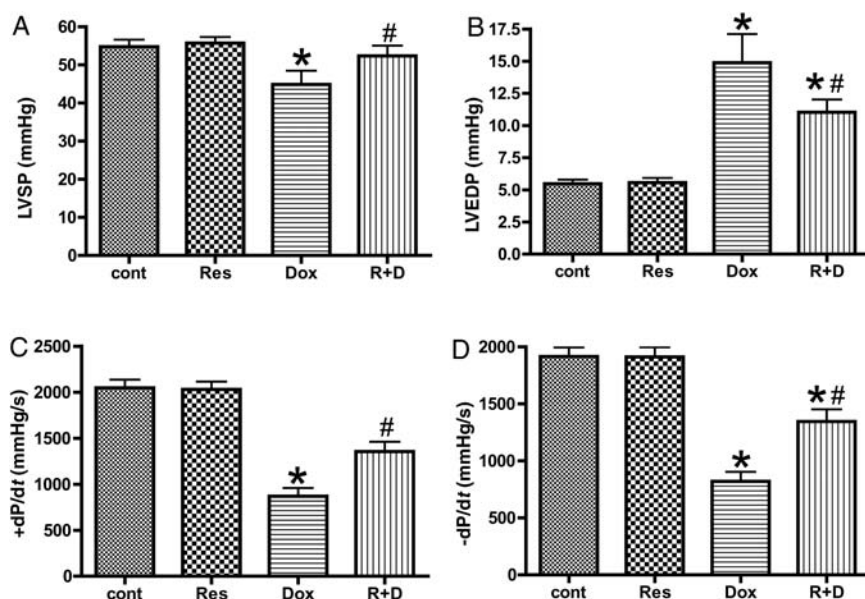


Figure 2 RES attenuated DOX-induced LV dysfunction. The mice were randomized into four groups (10 mice each) with similar body weight, a normal diet-fed group (control), a normal diet plus RES group (RES), a DOX-treated group (DOX), and a DOX-treated RES group (R + D). Seven weeks after the DOX administration, left ventricular performance was measured in mice anaesthetized by intraperitoneal injection of 10% chloral hydrate (2.5 mL/kg). The haemodynamic variables between different treatment groups are shown. (A) Changes of left ventricular systolic pressure (LVSP). (B) Left ventricular end-diastolic pressure (LVEDP). (C) The maximal slope of systolic pressure increment (+dP/dt). (D) The maximal slope of diastolic pressure decrement (−dP/dt). The values are shown as means + SD. * $P < 0.05$ vs. the control group; # $P < 0.05$ vs. the DOX group; $n = 6$.

significant decline in haemodynamic indices compared with the control group in LVSP (44.8 vs. 54.7 mmHg, $P < 0.05$; Figure 2A), LVEDP (14.9 vs. 5.5 mmHg, $P < 0.05$; Figure 2B), +dP/dt (870 vs. 2047 mmHg/s, $P < 0.05$; Figure 2C), and −dP/dt (821 vs. 1915 mmHg/s, $P < 0.05$; Figure 2D). However, the DOX-induced degeneration of LVSP, LVEDP, +dP/dt, and −dP/dt was significantly alleviated by RES in the R + D group compared with the DOX group ($P < 0.05$; Figure 2).

3.3 RES alleviated DOX-induced oxidative damage

As shown in Figure 3, compared with the control group, RES alone did not change the serum level of LDH, but DOX alone increased the serum LDH level by 1.42-fold over the control group. The serum LDH level in the combined treatment of RES and DOX was greatly decreased when compared with that in the DOX group (Figure 3A). Analogously, protein carbonyl content in heart homogenates were significantly elevated (2.26-fold vs. the control group) in the DOX treatment group, but significantly reduced after the combined treatment of RES and DOX (Figure 3B). In addition, DOX induced a 39.1% increase in MDA in heart homogenates, while there was only a 12.1% increase in the case of RES supplement treatment (Figure 3C).

3.4 RES attenuated DOX-induced myocardial apoptosis

Apoptosis was measured by TUNEL assay. As shown in Figure 4, following 7 weeks of DOX treatment, a significant increase (11.8%,

apoptotic index) in the apoptotic (TUNEL-positive) cells was detected (Figure 4C), but it was alleviated (7.0%, apoptotic index) by combined treatment with RES (Figure 4D).

3.5 RES induced SIRT1 protein overexpression and weakened p53 protein acetylation

To determine whether SIRT1 is involved in doxorubicin-induced myocardial apoptosis, we compared SIRT1 protein levels in the four groups (Figure 5A). Moderate levels of SIRT1 were detected in the control group, and SIRT1 protein level was slightly increased by treatment with DOX or RES alone, but a markedly increased SIRT1 protein level was detected in the R + D group. In addition, co-immunoprecipitation assays showed that SIRT1 and p53 were co-immunoprecipitated with each other in the four groups (Figure 5B). Further study in acetylation assays found that p53 protein was weakly acetylated in the control and RES groups, but markedly acetylated in the DOX treatment group. RES weakened p53 protein acetylation in the R + D group mice (Figure 5C).

3.6 RES weakened DOX-induced p53 DNA-binding activity and Bax overexpression

That acetylation of p53 stimulates its DNA-binding activity *in vivo* has been described previously.¹⁰ Therefore, we investigated whether RES could affect p53-stimulated DNA binding to the p53-responsive element within the *Bax* promoter using EMSA analysis. It was found that DOX treatment resulted in enhanced p53-stimulated DNA

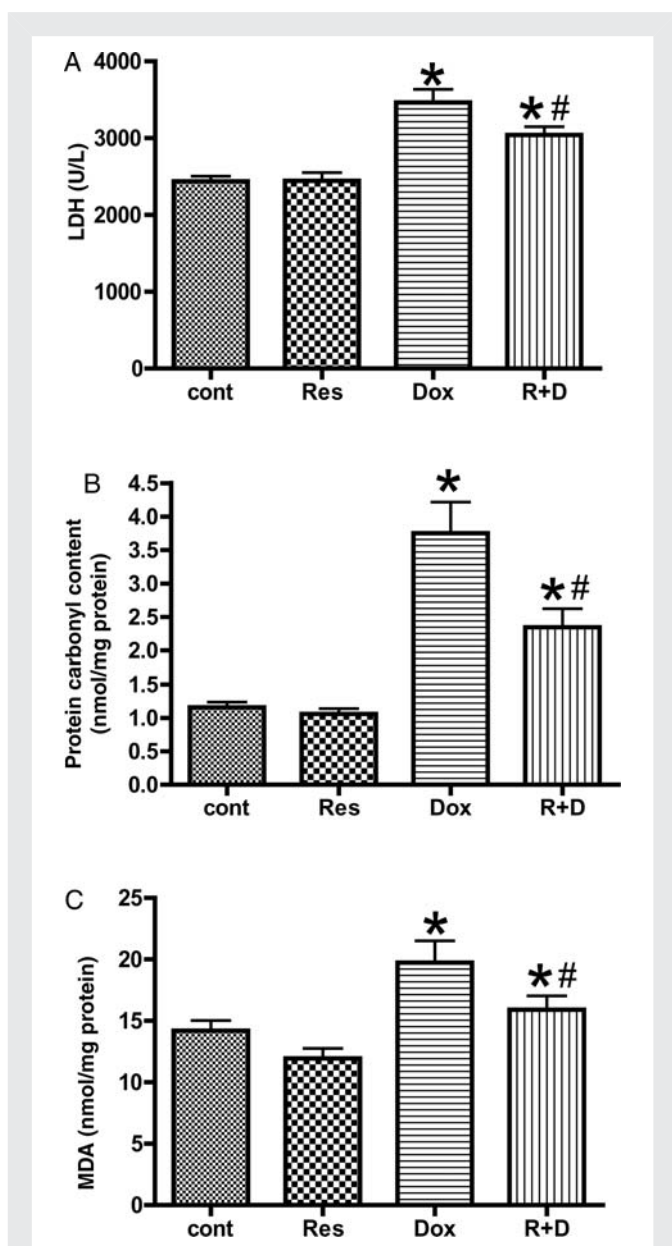


Figure 3 RES treatments alleviated DOX-induced oxidative damage. The mice were treated with saline, DOX, RES, and RES + DOX. Changes of serum lactate dehydrogenase (A), protein carbonyl content (B), and malondialdehyde (MDA) content (C) in the heart homogenates were detected. The values are shown as means \pm SD. * $P < 0.05$ vs. the control group; # $P < 0.05$ vs. the DOX group; $n = 6$.

binding to the p53-responsive element within the *Bax* promoter, but DOX treatment supplemented with RES could weaken this effect (Figure 6A). Additionally, we found that treatment with DOX increased the expression of the pro-apoptotic *Bax* protein. This effect of DOX could also be alleviated by RES in the R + D group (Figure 6B).

3.7 RES suppressed DOX-induced cytochrome *c* release from mitochondria

Cytochrome *c* contents in the mitochondria and cytosol after the DOX treatment were measured by western blot. To ensure there

was no cross-contamination between the cytosolic and mitochondrial fractions caused by the isolation procedure, VDAC in each fraction was measured. DOX significantly increased the cytosolic concentration of cytochrome *c*, with a concomitant decrease in the mitochondria, as shown in Figure 6C. Quantitative data showed that the cytosolic concentration of cytochrome *c* was increased from 4.3 to 41.6% of the total cellular concentration in the cardiomyocytes of DOX-treated mice. This effect was significantly suppressed in the R + D group (Figure 6D). The DOX-induced release of cytochrome *c* from mitochondria was inhibited by 62.9% in the R + D group (Figure 6C and D).

4. Discussion

RES is a polyphenol mainly found in red wines and is well known for its antioxidant properties.¹¹ To determine the potential protective action of RES against the cardiotoxic effect of DOX, we developed a mouse model of DOX-induced cardiotoxicity *in vivo*. DOX remarkably depressed left ventricular function, induced mitochondrial cytochrome *c* release, and decreased heart weight, body weight, and ratio of heart weight to body weight in mice, but inversely increased the number of apoptotic myocardial cells and the level of serum lactate dehydrogenase, protein carbonyl, and MDA in the myocardium. However, RES administration at 15 mg/kg per day for 7 weeks was effective in protecting the mice against DOX-induced cardiotoxicity. These results proved the hypothesis that RES could attenuate DOX-induced cardiotoxicity.

Previous studies have found that apoptotic cell death is a key component in DOX-induced cardiotoxicity.^{12–15} RES can reduce cardiomyocyte apoptosis caused by various forms of damage, such as hypoxia¹⁶ and ischaemia–reperfusion injury.¹⁷ In the present study, the DOX-induced apoptotic index decreased from 11.8 to 7.0% after RES treatment (Figure 4). We believed that the protective effect of RES against DOX-induced cardiotoxicity was related to a decreased number of apoptotic cardiomyocytes.

Some researchers have reported that RES induced an anti-apoptotic signal for the protection of the heart.¹⁸ Moreover, the beneficial effects of RES include its ability to increase the activity of the anti-ageing gene *SIRT1*.¹⁹ *SIRT1* is implicated in various cellular functions, ranging from gene silencing, the control of the cell cycle, and apoptosis to energy homeostasis.²⁰ Most importantly, *SIRT1* could deacetylate p53 and attenuate its ability to transactivate its downstream target genes, such as *p21* for cell-cycle arrest and *Bax* for apoptosis.^{21,22} As the p53 protein has several acetylation sites, whose hyperacetylation stabilized and activated itself to trigger the apoptosis,^{23,24} it plays an important role in DOX-induced cardiomyocyte apoptosis.²⁵ We hypothesized that the protective effect of RES against DOX-induced cardiotoxicity might involve the activation of *SIRT1* and subsequent deacetylation and inactivation of p53. As shown in Figure 5A, moderate levels of *SIRT1* were detected in the control group, and the *SIRT1* protein level was slightly increased by DOX or RES treatment, but a markedly increased *SIRT1* protein level was detected in the R + D group. These results indicated that RES up-regulates *SIRT1* protein expression. The possible interaction of *SIRT1* and p53 was studied using a co-immunoprecipitation assay. It was shown that *SIRT1* and p53 were co-immunoprecipitated with each other (Figure 5B). DOX treatment dramatically increased p53 acetylation in myocardium, but this was alleviated by combined treatment with DOX and RES (Figure 5C). Then, acetylation-mediated p53 binding activity to the p53-responsive

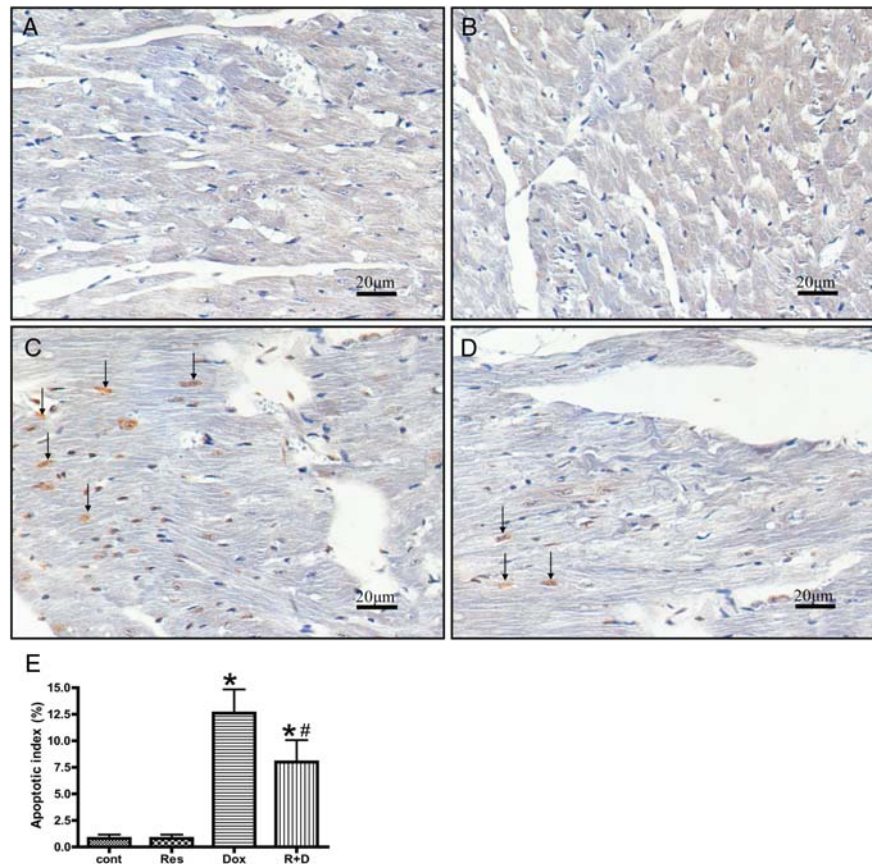


Figure 4 Apoptotic myocytes from mouse myocardium were detected by TUNEL staining. Treatment with RES reduced myocardial TUNEL staining in DOX-treated mice. Representative photomicrographs are shown demonstrating TUNEL staining of heart sections from the control group (A), the RES group (B), the DOX group (C), and the R + D group (D). TUNEL-positive cells are indicated by brown staining, and the TUNEL-positive cardiac myocytes are indicated by arrows. (E) Histogram showing the quantitative analysis of TUNEL-positive cells. * $P < 0.05$ vs. the control group; # $P < 0.05$ vs. the DOX group; $n = 3$.

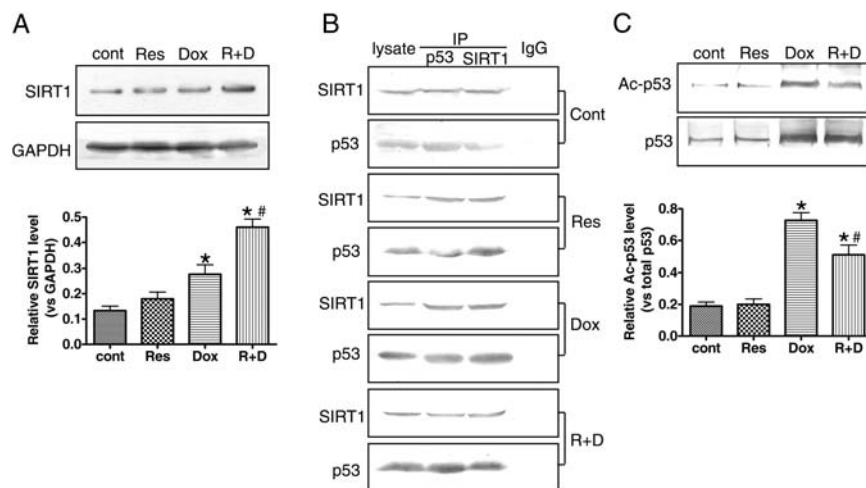


Figure 5 RES up-regulated the expression of SIRT1 and inhibited the acetylation of p53. (A) SIRT1 protein expression in the heart of Balb/c mouse was examined by western blot. (B) Co-immunoprecipitation assay showed that SIRT1 and p53 were co-immunoprecipitated with each other. (C) The heart homogenates were subjected to immunoprecipitation with p53 antibody, and acetylated p53 was detected by western blot with an acetylated lysine antibody. * $P < 0.05$ vs. the control group; # $P < 0.05$ vs. the DOX group; $n = 3$.

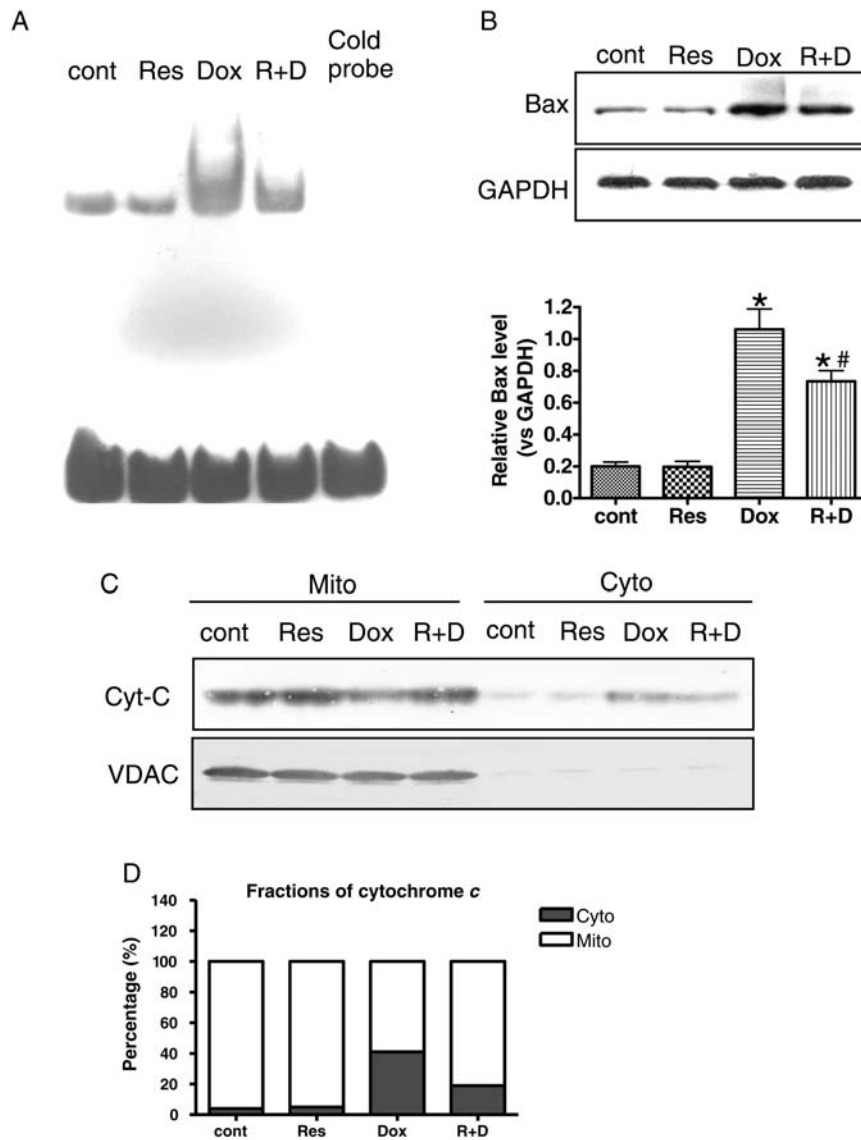


Figure 6 RES attenuated DOX-induced activation of p53 DNA binding, transcriptional activity and release of cytochrome c. (A) Binding activity of p53 to *Bax* promoter sequence was detected by EMSA. The oligonucleotide corresponding to the p53 binding site of the *Bax* promoter sequence and nuclear extract of heart tissue were used. (B) *Bax* expression level was detected by western blot with anti-*Bax* polyclonal antibody, and GAPDH level served as the loading control. (C) Cytosolic and mitochondrial cytochrome c distribution were studied by western blot. Data are representative of three independent experiments. (D) Quantitative analysis of cytochrome c release from the mitochondria into the cytosol. Mito, mitochondrial; Cyto, cytosolic. * $P < 0.05$ vs. the control group; # $P < 0.05$ vs. the DOX group; $n = 3$.

element within the *Bax* promoter was further observed. It was found that DOX treatment resulted in enhanced p53-stimulated DNA binding to the p53-responsive element within the *Bax* promoter. This enhancement was weakened by the combined treatment of RES (Figure 6A). Consistent with this result, the *Bax* protein level was also increased in the DOX treatment group, while combined treatment with DOX and RES decreased *Bax* expression when compared with the DOX group (Figure 6B). These results indicated that RES protected DOX-induced cardiomyocyte apoptosis in mice through SIRT1-modulated p53-mediated apoptosis by a transcription-dependent pathway. However, as increasing evidence suggests that p53 can function independent of its transcription activation by directly acting on

mitochondria in the cardiomyocyte response to DOX,²⁶ mediated by the release of cytochrome c from the mitochondrial intramembrane,²⁷ we also checked the effect of RES on cytochrome c release. The data (Figure 6C and D) showed that the DOX-induced cytochrome c release from mitochondria was inhibited by RES. This indicated that the cardioprotective effect of RES was also related to the inhibition of the transcription-independent pro-apoptotic pathway of p53.

In summary, our data showed that RES protected against DOX-induced cardiotoxicity, as indicated by decreased elevation of serum LDH, protein carbonyl formation, MDA content in the myocardium, and cardiomyocyte apoptosis. The protective effect of RES was related to the up-regulation of SIRT1, resultant deacetylation of

p53, and reduced p53-mediated cardiomyocyte apoptosis by transcription-dependent and -independent mechanisms.

Conflict of interest: none declared.

Funding

This work was supported by grants from the Major National Basic Research Program of China (no. 2007CB512007).

References

- Chua CC, Liu X, Gao J, Hamdy RC, Chua BH. Multiple actions of pifithrin- α on doxorubicin-induced apoptosis in rat myoblastic H9c2 cells. *Am J Physiol Heart Circ Physiol* 2006;**290**:H2606–H2613.
- Nakamura T, Ueda Y, Juan Y, Katsuda S, Takahashi H, Koh E. Fas-mediated apoptosis in adriamycin-induced cardiomyopathy in rats: in vivo study. *Circulation* 2000;**102**:572–578.
- Das DK, Maulik N. Resveratrol in cardioprotection: a therapeutic promise of alternative medicine. *Mol Interv* 2006;**6**:36–47.
- Mukherjee S, Lekli I, Gurusamy N, Bertelli AA, Das DK. Expression of the longevity proteins by both red and white wines and their cardioprotective components, resveratrol, tyrosol, and hydroxytyrosol. *Free Radic Biol Med* 2009;**46**:573–578.
- Danz EDB, Skramsted J, Henry N, Bennett JA, Keller RS. Resveratrol prevents doxorubicin cardiotoxicity through mitochondrial stabilization and the Sirt1 pathway. *Free Radic Biol Med* 2009;**46**:1589–1597.
- Howitz KT, Bitterman KJ, Cohen HY, Lamming DW, Lavu S, Wood JG *et al*. Small molecule activators of sirtuins extend *Saccharomyces cerevisiae* lifespan. *Nature* 2003;**425**:191–196.
- Liu L, Zhang X, Qian B, Min X, Gao X, Li C *et al*. Over-expression of heat shock protein 27 attenuates doxorubicin-induced cardiac dysfunction in mice. *Eur J Heart Fail* 2007;**9**:762–769.
- Elberry AA, Abdel-Naim AB, Abdel-Sattar EA, Nagy AA, Mosli HA, Mohamadin AM *et al*. Cranberry (*Vaccinium macrocarpon*) protects against doxorubicin-induced cardiotoxicity in rats. *Food Chem Toxicol* 2010;**48**:1178–1184.
- Kawamura N, Kubota T, Kawano S, Monden Y, Feldman AM, Tsutsui H *et al*. Blockade of NF- κ B improves cardiac function and survival without affecting inflammation in TNF- α -induced cardiomyopathy. *Cardiovasc Res* 2005;**66**:520–529.
- Ivanov GS, Ivanova T, Kurash J, Ivanov A, Chuiikov S, Gizatullin F *et al*. Methylation-acetylation interplay activates p53 in response to DNA damage. *Mol Cell Biol* 2007;**27**:6756–6769.
- Baur JA, Sinclair DA. Therapeutic potential of resveratrol: the *in vivo* evidence. *Nat Rev Drug Discov* 2006;**5**:493–506.
- Kumar D, Kirshenbaum LA, Li T, Danelisen I, Singal PK. Apoptosis in adriamycin cardiomyopathy and its modulation by probrucol. *Antioxid Redox Signal* 2001;**3**:135–145.
- Ueno M, Kakinuma Y, Yuhki K, Murakoshi N, Iemitsu M, Miyauchi T *et al*. Doxorubicin induces apoptosis by activation of caspase-3 in cultured cardiomyocytes in vitro and rat cardiac ventricles in vivo. *J Pharmacol Sci* 2006;**101**:151–158.
- Li K, Sung RY, Huang WZ, Yang M, Pong NH, Lee SM *et al*. Thrombopoietin protects against in vitro and in vivo cardiotoxicity induced by doxorubicin. *Circulation* 2006;**113**:2211–2220.
- Nozaki N, Shishido T, Takeishi Y, Kubota I. Modulation of doxorubicin-induced cardiac dysfunction in toll-like receptor-2-knockout mice. *Circulation* 2004;**110**:2869–2874.
- Chen CJ, Yu W, Fu YC, Wang X, Li JL, Wang W. Resveratrol protects cardiomyocytes from hypoxia-induced apoptosis through the SIRT1–FoxO1 pathway. *Biochem Biophys Res Commun* 2009;**378**:389–393.
- Lekli I, Szabo G, Juhasz B, Das S, Das M, Varga E *et al*. Protective mechanisms of resveratrol against ischemia-reperfusion-induced damage in hearts obtained from Zucker obese rats: the role of GLUT-4 and endothelin. *Am J Physiol Heart Circ Physiol* 2008;**294**:H859–H866.
- El-Mowafy AM, White RE. Resveratrol inhibits MAPK activity and nuclear translocation in coronary artery smooth muscle: reversal of endothelin-1 stimulatory effects. *FEBS Lett* 1999;**451**:63–67.
- Hall SS. Longevity research. In vino vitalis? Compounds activate life-extending genes. *Science* 2003;**301**:1165.
- Yamamoto H, Schoonjans K, Auwerx J. Sirtuin functions in health and disease. *Mol Endocrinol* 2007;**21**:1745–1755.
- Luo J, Nikolaev AY, Imai S, Chen D, Su F, Shiloh A *et al*. Negative control of p53 by Sir2 α promotes cell survival under stress. *Cell* 2001;**107**:137–148.
- Vaziri H, Dessain SK, Ng Eaton E, Imai SI, Frye RA, Pandita TK *et al*. hSIR2(SIRT1) functions as an NAD-dependent p53 deacetylase. *Cell* 2001;**107**:149–159.
- Appella E, Anderson CV. Post-translational modifications and activation of p53 by genotoxic stresses. *Eur J Biochem* 2001;**268**:2764–2772.
- Brooks CL, Gu W. Ubiquitination, phosphorylation and acetylation: the molecular basis for p53 regulation. *Curr Opin Cell Biol* 2003;**15**:164–171.
- Liu X, Chua CC, Gao J, Chen Z, Landy CL, Hamdy R *et al*. Pifithrin- α protects against doxorubicin-induced apoptosis and acute cardiotoxicity in mice. *Am J Physiol Heart Circ Physiol* 2004;**286**:H933–H939.
- Nithipongvanitch R, Ittarat W, Cole MP, Tangpong J, Clair DK, Oberley TD. Mitochondrial and nuclear p53 localization in cardiomyocytes: redox modulation by doxorubicin (Adriamycin)? *Antioxid Redox Signal* 2007;**9**:1001–1008.
- Erster S, Moll UM. Stress-induced p53 runs a transcription-independent death program. *Biochem Biophys Res Commun* 2005;**331**:843–850.